



CHORUS

This is the accepted manuscript made available via CHORUS. The article has been published as:

Observation of Fourier transform limited lines in hexagonal boron nitride

A. Dietrich, M. Bürk, E. S. Steiger, L. Antoniuk, T. T. Tran, M. Nguyen, I. Aharonovich, F. Jelezko, and A. Kubanek

Phys. Rev. B **98**, 081414 — Published 31 August 2018

DOI: [10.1103/PhysRevB.98.081414](https://doi.org/10.1103/PhysRevB.98.081414)

Observation of Fourier Transform Limited Lines in Hexagonal Boron Nitride

A. Dietrich¹, M. Bürk¹, E. S. Steiger¹, L. Antoniuk¹, T. T. Tran², M. Nguyen², I. Aharonovich², F. Jelezko^{1,3}, A. Kubanek^{1,3}
¹ *Institute for Quantum Optics, Ulm University, D-89081 Ulm, Germany*
² *Institute of Biomedical Materials and Devices, Faculty of Science, University of Technology Sydney, Ultimo, New South Wales 2007, Australia*
³ *Center for Integrated Quantum Science and Technology (IQst), Ulm University, D-89081 Ulm, Germany*

(Dated: July 19, 2018)

Single defect centers in layered hexagonal Boron Nitride (hBN) are promising candidates as single photon sources for quantum optics and nanophotonics applications. However, until today spectral instability hinders many applications. Here, we perform resonant excitation measurements and observe Fourier Transform (FT) limited linewidths down to ≈ 50 MHz. We investigated optical properties of more than 600 single photon emitter (SPE) in hBN. The SPEs exhibit narrow zero-phonon lines (ZPL) distributed over a spectral range from 580 nm to 800 nm and with dipole-like emission with high polarization contrast. Finally, the emitters withstand transfer to a foreign photonic platform - namely a silver mirror, which makes them compatible with photonic devices such as optical resonators and paves the way to quantum photonics applications.

DOI: XXXXXXXX

Single photon emitters (SPEs) are prime building blocks for a variety of applications in integrated quantum photonics, quantum information processing and fundamental studies of quantum optics [1–6]. Availability of Fourier Transform (FT) limited photons - without spectral diffusion, dephasing or competing phonon processes, is required for the majority of these applications [1–6]. Single-photon sources with FT limited lines have been demonstrated with atoms or ions in gas phase, organic molecules as well as with solid state systems such as quantum dots and color centers in diamond [7, 8]. While those systems have been explored in some of the pioneering nanophotonic experiments, a bright, robust FT limited source that is easily accessible remains a challenge. In this regard a new emerging class of SPEs are embedded in two-dimensional host materials such as hBN that offer high brightness and may enable novel architectures for integrated quantum technologies [9, 10]. The optical properties are promising with high photostability [11], high brightness [12–14], large Debye Waller factor [15, 16], good polarization contrast [17–19], spectral tunability [14, 15], stable optical lines as narrow as $45 \mu\text{eV}$ at cryogenic temperatures [16, 20] and, very recently, resonant excitation with lines measured in photoluminescence excitation (PLE) as narrow as 1 GHz [21]. However, the close proximity of the SPE to the host surface makes it susceptible to spectral instability, typically exhibiting, blinking, rapid spectral diffusion and pure dephasing rates much larger than the population decay rates and therefore ZPLs much broader than the natural linewidth [22].

In this work, we demonstrate spectrally stable, single-photon emission from defect center in hBN under resonant excitation without significant spectral diffusion for as long as 30 seconds. We performed a detailed study of 627 different defect centers in hBN with central emission

wavelength from 580 nm to 800 nm. [17, 18, 21, 23–25]. Resonant excitation reveals linewidths within the FT limit of approx. 55 ± 10 MHz. Our investigated platform consists of two-dimensional hBN flakes mounted on a silver mirror which enables direct integration into photonic structures such as optical resonators, for example, for spin-photon interfaces with Purcell-enhanced, lifetime-limited, single-photon emission.

The hBN flakes are cooled in a continuous-flow cryostat to liquid helium temperature, see Fig. 1(a). The excitation and emission polarization is extracted by a linear polarizer and a λ -half wave plate probing the incident or emitted polarization via spectrometer and/or via APD counts.

For resonant excitation we use a CW Matisse DS Dye laser system, which has a mode hop-free scanning range of >40 GHz and a line-width of <250 kHz. The wavelength of the laser is monitored via a wave meter from High Finesse with 500 kHz resolution and acquisition frequency up to 600 Hz. Photo Luminescence Excitation (PLE) is measured by detecting the phonon-sideband (PSB) emission while the direct laserlight is blocked with a LP Filter.

We evaluate emission spectra from many different SPEs and measure second-order autocorrelation function in a Hanbury-Brown and Twiss setup (HBT) with $g^2(\tau = 0) < 0.5$ proofing the single photon character of the SPE, see Fig. 1(c). The data fit is based on $g^2(\tau)$ model for two level system

$$g^2(\tau) = 1 - a \cdot e^{|\tau|/\tau_0}. \quad (1)$$

Various sites have lifetimes in the range of $\tau_0 \approx 1.53 - 2.88$ ns resulting in natural linewidth of $\Gamma \approx 55 - 84$ MHz, in agreement to previous results [15, 21, 22]. A background signal originating from fluorescence of the silver mirror under off-resonant excitation leads to a signal-to-

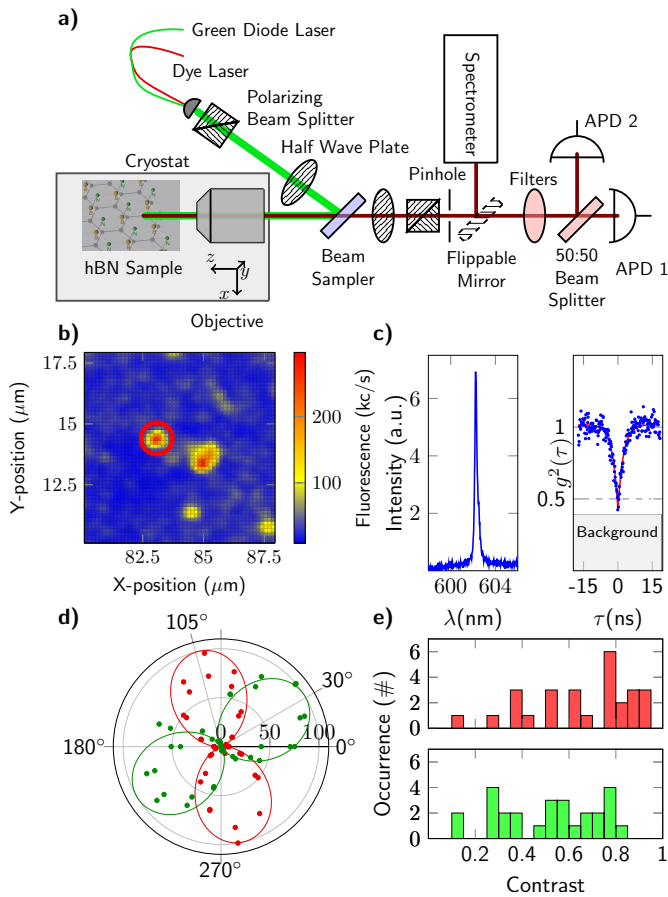


FIG. 1. (a) Experimental Setup. The hBN sample is cooled to liquid helium temperatures of ≈ 5 K in a continuous flow cryostat and investigated via a custom-built confocal microscope with a high NA Objective of 0.9. All PL and polarization measurements are performed under identical conditions, in off-resonant excitation with a 532 nm green diode laser and with a power of up to $250 \mu\text{W}$ in front of the objective. A spectrometer with an maximal resolution of 16 GHz records the PL spectra with a acquisition time of 10 s and an HBT setup enables to extract second-order, photon correlations. For Polarization measurements we use additional polariser and a λ -half wave plate. Resonant excitation was performed using a CW Matisse DS Dye Laser. (b) Confocal scan (max. $200 \times 200 \mu\text{m}$) of the emitters in hBN flakes with off-resonant excitation. (c) Off-resonant spectrum and second-order correlation of the emitter marked in b). $g^2(0) = 0.42$ reveals single photon character of the SPE. Background subtraction, originating from a signal to noise ratio of ≈ 1.4 , results in $g^2(0) = 0.01$. The lifetime is then extrapolated to 2.37 ± 0.12 ns corresponding to a natural linewidth of $\approx 67.2 \pm 3.2$ MHz. (d) and (e) We find emission and excitation are misaligned by 75° . The polarization contrast of emission (red data) have an average 0.6 and for excitation (green data) 0.5.

noise ratio of ≈ 1.4 . Background subtraction results in $g^2(\tau) = 0.01$.

As described in reference [26] linear polarized or circular polarized dipoles are expected from a symmetry based group theory approach of the defect centers. We proof

the polarisation properties by measuring the emission polarization, red data, for the emitter at 602 nm emission wavelength in fig 1 (d), with a contrast as high as 0.9 and with an average of 0.6 from statistics of 28 emitter in data shown in red fig 1 (e). The contrast is defined as :

$$C = \frac{I_{max} - I_{min}}{I_{max} + I_{min}} \quad (2)$$

Deviation from perfect polarization contrast may originate from non-perfect horizontal alignment of the hBN flakes with respect to the substrate. We infer the polarization-dependence for the off-resonant excitation by placing the polarizer in the excitation path and recording the fluorescence depending on the excitation angle (see Fig. 1a). The polarization in off-resonant excitation results in a significantly reduced contrast of on average 0.5 reflecting the incoherent process and indicating that polarization is not preserved in phonon-assisted excitation.

PL spectra are recorded for 627 individual ZPL lines, distributing from 580 nm to 800 nm, see Fig. 2(a). The ZPL emission frequencies cluster in four distinct positions, with peaks at 590 nm, 630 nm, 670 nm and 700 nm with an overall decreasing occurrence with increasing wavelength. Another cluster is indicated at 750 nm. Each cluster could originate from a specific emitter composition with an inhomogeneous spectral linewidth of about $\text{FWHM} \approx 25$ nm [27]. In-depth knowledge on the SPEs formation could be gained by comparison with ab-initio calculations as developed in references [25, 28]. The grouping into four distinct regions can be correlated to the simulated compositions of the defects as depicted in Fig. 2 bottom. The high energy emission is likely to correlate to the neutrally charged $N_B V_N$ defect [25, 28]. The lower energy emission is likely to correlate to the proposed carbon related defects, the positively charged ($V_N C_B$) [26] and the $C_N V_B$ defect [25]. While our work is beyond the scope of concretely isolating the selected defect, we note that these defects have similar crystallographic symmetry and therefore are expected to yield similar resonant excitation behavior. Our data could be used to refine and calibrate future ab-initio calculations. The observed spectral diffusion is in accord with the calculated structure that suggests a persistent dipole moment.

In the inset of Fig. 2 we plot the histogram of the SPEs linewidths, before an after an additional annealing at 500°C for 1 hr. Before annealing the average linewidths of 612 individual sites is 339 GHz, while after annealing the linewidth reduces to 213 GHz. (see inset of Fig. 2). All measurements were recorded under $250 \mu\text{W}$ of 532 nm excitation, using a spectrometer resolution of 16 GHz and 10 seconds acquisition time. The improved linewidth can be explained by elimination of chemical residue on the

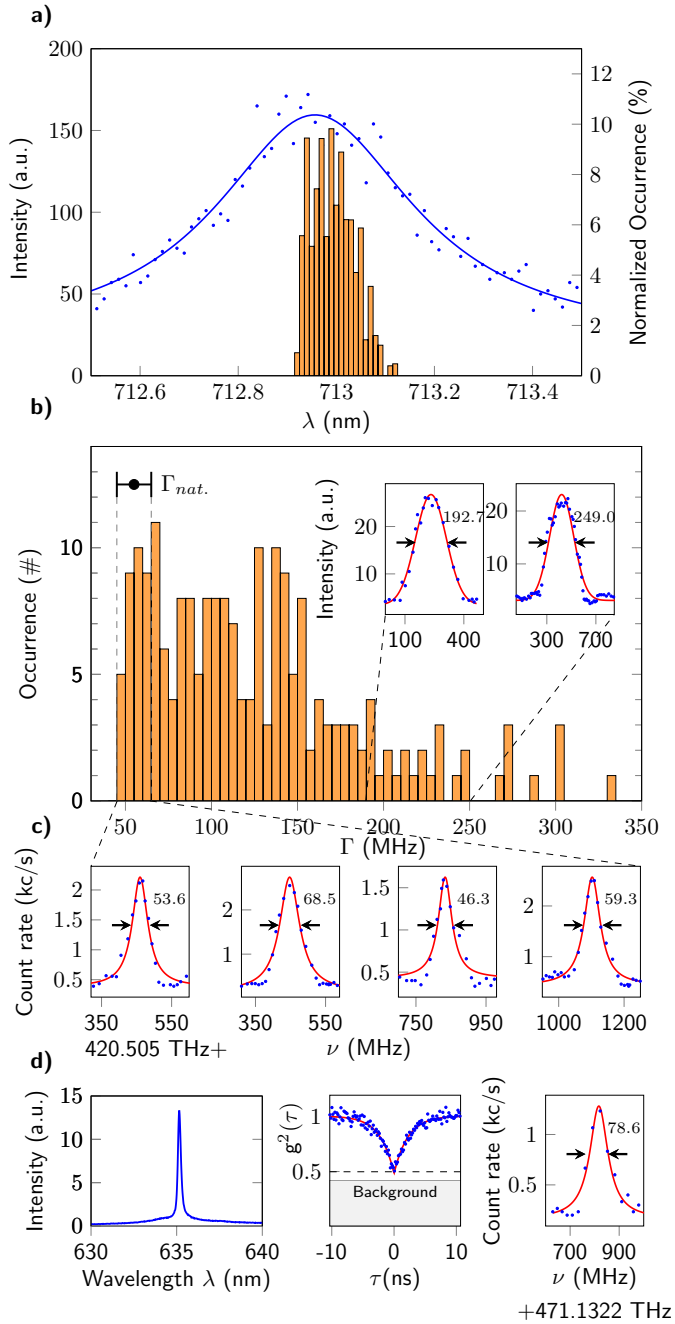


FIG. 4. (a) The PL spectrum (blue data) has an inhomogeneous linewidth of $\approx 293.39 \pm 8.13$ GHz. The histogram of 204 PLE lines measured for the same emitter over a range of 200 GHz reveals an inhomogeneous linewidth of $\approx 67.5 \pm 9.5$ GHz. (b) The homogeneous linewidth extracted from more than 204 PLE linescans of the same emitter unfolds 124.5 ± 60.5 MHz. The large variance hints at ongoing dynamics on the second timescale of the performed scans. (c) About 39 lines of that specific emitter are fitted with a Lorentzian lineshape and lie within the error margin of the natural linewidth of 55 ± 10 MHz. For details on the evaluation see supplementary material at [36]. (d) We reproduced FT limited lines on a second emitter with emission wavelength at 635 nm with a natural linewidth of $\Gamma_{nat} = (60.1 \pm 3.4)$ MHz inferred from second order correlation function and a time constant of 0.015 s.

bleaching. Eventually very long periods of stable fluorescence occur for many seconds which we attribute to slowly fluctuating, trapped carrier-induced Stark shifts followed by large spectral jumps as reported in [39]. Such periods of stable fluorescence enable us to perform resonant confocal scans without any significant change in the fluorescence signal, see inset Fig. 3(c). Detailed time-resolved statistics of the blinking timescale is unfolded by a histogram of the 'ON' times over their occurrence with a binning of 0.2 s in Fig. 3(c). A fit with an exponential decay reveals a single time constant of $\tau = 0.378 \pm 0.017$ s.

In order to record linewidth in resonant excitation we perform PLE line scans faster than characteristic diffusion time $\tau = 0.378$ s. The slowest applied scanning speed of the resonant laser is about 133 MHz/s with a recording frequency of 50 Hz. We obtained the best signal to noise ratio for 4-6 μ W excitation power in front of the objective, while we made sure to be well below saturation.

Several PLE scans performed over range of 200 GHz of the same SPE emitting at 713 nm uncover the histogram displayed in Fig. 4(a). Scans beyond this 200 GHz revealed no signal. We normalize the statistics of occurrences in Fig. 4(a) right axis, taking into account the number of scans per bin (6 GHz). The normalized PLE statistic discloses a spectral width of $\approx 67.5 \pm 9.5$ GHz much narrower than the inhomogeneous PL linewidth of $\approx 293.39 \pm 8.13$ GHz (blue data and Gaussian fit in Fig. 4(a)). We filtered out all data which showed blinking during laser scanning. Ongoing blinking and diffusion dynamics hinder further investigations on the fine structure, necessitating additional surface treatment and passivation techniques. The lifetime of this line is ≈ 2.88 ns giving a FT limited linewidth of $\Gamma_{nat.} = 55.26 \pm 0.19$ MHz. While the homogeneous linewidth of 124.5 MHz is still more than twice as large as the FT limited linewidth the large variance of 60.5 MHz after averaging over all 204 lines indicates on-going dynamics on the timescale of the resonant laser scan. Details of the linewidth statistic in Fig. 4(b) shows a vast spread with linewidth up to 200 MHz. Two examples of the broadened resonant lines are shown in the inset. Note that these lines are fit well with Gaussian function. We suspect that the diffusion dynamics discussed above, causes this spectral broadening. Nevertheless, about 39 lines out of all 204 lines are within the error margin of 10 MHz of the natural linewidth. We fitted the lines with a Lorentz function and four example lines are shown in Fig. 4(c), displaying FT limited lines with linewidth of $46 - 60 \pm 10$ MHz. The uncertainty of 10 MHz arises from the systematic error of the measurement and the evaluation algorithm. We manifest the FT limited line with a second SPE that exhibits a ZPL at 635 nm (fig. 4(d)). Second order autocorrelation measurement extracted to zero excitation power [40] with similar background yield a natural linewidth of

$\tau_{nat} = (60.1 \pm 3.4)$ MHz (see supplemental material at [36]). This natural linewidth can be compared with PLE measured linewidth of (78.6 ± 1.3) MHz see fig 4(d)).

In summary, we have demonstrated FT limited, single-photon emission from two different defect centers in hBN without significant spectral diffusion or spectral instability for as long as 30 seconds. Conservative extrapolation from the reported count rates of ≈ 2000 counts/sec, measured well below saturation and detecting only small fraction of the sideband emission, yields indistinguishable single photon emission rates much larger than 20000 counts/sec in the current setting assuming a Debye-Waller factor of 0.82 as reported in [12].

The investigated platform consists of hBN flakes placed on a silver mirror and opens new perspective for resonance fluorescence experiments or investigations of mirror image interactions. The architecture demonstrates the compatibility with photonic platforms, in particular optical resonators, for Purcell-enhanced single photon emission facilitating indistinguishable photon rates up to GHz rates. Some SPE in hBN could potentially inhere long spin coherence time [28, 41]. In addition, our detailed investigations of more than 627 SPEs in hBN give new input for theoretical predictions of the defects composition by comparing ab-initio simulations [26] with the reported emission frequencies.

A.K. and A.D. acknowledge S. Häußler and M. Metsch for fruitful discussion and experimental support. AK acknowledges the generous support of the DFG, the Carl-Zeiss Foundation, IQST, the Wissenschaftler-Rückkehrprogramm GSO/GZS. F.J. acknowledges support of the DFG, BMBF, VW Stiftung and EU (ERC, DIADEMS). I.A. acknowledges the generous support of the Alexander van Humboldt foundation, and the Asian Office of Aerospace Research & Development (grant # FA2386-17-1-4064), the Office of Naval Research Global (grant # N62909-18-1-2025) and the Australian Research Council (DP180100077). Experiments performed for this work were operated using the Qudi software suite [42].

-
- [1] D. L. Moehring, P. Maunz, S. Olmschenk, K. C. Younge, D. N. Matsukevich, L.-M. Duan, and C. Monroe, *Nature* **449**, 68 (2007).
 - [2] S. Ritter, C. Nölleke, C. Hahn, A. Reiserer, A. Neuzner, M. Uphoff, M. Mücke, E. Figueroa, J. Bochmann, and G. Rempe, *Nature* **484**, 195 (2012).
 - [3] H. Bernien, B. Hensen, W. Pfaff, G. Koolstra, M. S. Blok, L. Robledo, T. H. Taminiau, M. Markham, D. J. Twitchen, L. Childress, and R. Hanson, *Nature* **497**, 86 (2013).
 - [4] T. Legero, T. Wilk, M. Hennrich, G. Rempe, and A. Kuhn, *Physical Review Letters* **93**, 070503 (2004).
 - [5] R. Lettow, Y. L. A. Rezus, A. Renn, G. Zumofen, E. Ikonen, S. Götzinger, and V. Sandoghdar, *Physical Review Letters* **104**, 123605 (2010).
 - [6] A. Sipahigil, M. L. Goldman, E. Togan, Y. Chu, M. Markham, D. J. Twitchen, A. S. Zibrov, A. Kubanek, and M. D. Lukin, *Physical Review Letters* **108**, 143601 (2012).
 - [7] B. Lounis and M. Orrit, *Reports on Progress in Physics* **68**, 1129 (2005).
 - [8] P. Senellart, G. Solomon, and A. White, *Nature Nanotechnology* **12**, 1026 (2017).
 - [9] A. W. Schell, H. Takashima, T. T. Tran, I. Aharonovich, and S. Takeuchi, *ACS Photonics* **4**, 761 (2017).
 - [10] T. T. Tran, D. Wang, Z.-Q. Xu, A. Yang, M. Toth, T. W. Odom, and I. Aharonovich, *Nano Letters* **17**, 2634 (2017).
 - [11] M. Kianinia, B. Regan, S. A. Tawfik, T. T. Tran, M. J. Ford, I. Aharonovich, and M. Toth, *ACS Photonics* **4**, 768 (2017).
 - [12] T. T. Tran, K. Bray, M. J. Ford, M. Toth, and I. Aharonovich, *Nature Nanotechnology* **11**, 37 (2016).
 - [13] L. J. Martinez, T. Pelini, V. Waselowski, J. R. Maze, B. Gil, G. Cassabo, and V. Jacques, *Physical Review B* **94**, 121405 (2016).
 - [14] G. Grosso, H. Moon, B. Lienhard, S. Ali, D. K. Efetov, M. M. Furchi, P. Jarillo-Herrero, M. J. Ford, I. Aharonovich, and D. Englund, *Nature Communications* **8**, 705 (2017).
 - [15] T. T. Tran, C. Elbadawi, D. Totnjanian, C. J. Lobo, G. Grosso, H. Moon, D. R. Englund, M. J. Ford, I. Aharonovich, and M. Toth, *ACS Nano* **10**, 7331 (2016).
 - [16] X. Li, G. D. Shepard, A. Cupo, N. Camporeale, K. Shayan, Y. Luo, V. Meunier, and S. Strauf, *ACS Nano* **11**, 6652 (2017).
 - [17] N. R. Jungwirth, B. Calderon, Y. Ji, M. G. Spencer, M. E. Flatt, and G. D. Fuchs, *Nano Letters* **16**, 6052 (2016).
 - [18] N. Chejanovsky, M. Rezai, F. Paolucci, Y. Kim, T. Rendler, W. Rouabeh, F. Fvaro de Oliveira, P. Herlinger, A. Denisenko, S. Yang, I. Gerhardt, A. Finkler, J. H. Smet, and J. Wrachtrup, *Nano Letters* **16**, 7037 (2016).
 - [19] A. L. Exarhos, D. A. Hopper, R. R. Grote, A. Alkauskas, and L. C. Bassett, *ACS Nano* **11**, 3328 (2017).
 - [20] N. R. Jungwirth and G. D. Fuchs, *Physical Review Letters* **119**, 057401 (2017).
 - [21] T. T. Tran, M. Kianinia, M. Nguyen, S. Kim, Z.-Q. Xu, A. Kubanek, M. Toth, and I. Aharonovich, *ACS Pho-*

- tonics (2017), 10.1021/acsphotonics.7b00977.
- [22] B. Sontheimer, M. Braun, N. Nikolay, N. Sadzak, I. Aharonovich, and O. Benson, *Physical Review B* **96**, 121202 (2017).
- [23] T. T. Tran, C. Zachreson, A. M. Berhane, K. Bray, R. G. Sandstrom, L. H. Li, T. Taniguchi, K. Watanabe, I. Aharonovich, and M. Toth, *Physical Review Applied* **5**, 034005 (2016).
- [24] R. Bourrellier, S. Meuret, A. Tararan, O. Stphan, M. Kociak, L. H. G. Tizei, and A. Zobelli, *Nano Letters* **16**, 4317 (2016).
- [25] S. A. Tawfik, S. Ali, M. Fronzi, M. Kianinia, T. T. Tran, C. Stampfl, I. Aharonovich, M. Toth, and M. J. Ford, *Nanoscale* **9**, 13575 (2017).
- [26] M. Abdi, J.-P. Chou, A. Gali, and M. B. Plenio, arXiv:1709.05414 [cond-mat, physics:quant-ph] (2017), arXiv: 1709.05414.
- [27] N. Mendelson, Z.-Q. Xu, T. T. Tran, M. Kianinia, C. Bradac, J. Scott, M. Nguyen, J. Bishop, J. Froch, B. Regan, I. Aharonovich, and M. Toth, arXiv:1806.01199 [cond-mat, physics:physics] (2018), arXiv: 1806.01199.
- [28] M. Abdi, M.-J. Hwang, M. Aghtar, and M. B. Plenio, *Physical Review Letters* **119**, 233602 (2017).
- [29] A. G. F. Garcia, M. Neumann, F. Amet, J. R. Williams, K. Watanabe, T. Taniguchi, and D. Goldhaber-Gordon, *Nano Letters* **12**, 4449 (2012).
- [30] J. Wolters, N. Sadzak, A. W. Schell, T. Schröder, and O. Benson, *Physical Review Letters* **110**, 027401 (2013).
- [31] M. Pelton, *Nature Photonics* **9**, 427 (2015).
- [32] G. Kern, G. Kresse, and J. Hafner, *Physical Review B* **59**, 8551 (1999).
- [33] T. Tohei, A. Kuwabara, F. Oba, and I. Tanaka, *Physical Review B* **73**, 064304 (2006).
- [34] S. Reich, A. C. Ferrari, R. Arenal, A. Loiseau, I. Bello, and J. Robertson, *Physical Review B* **71**, 205201 (2005).
- [35] D. Snchez-Portal and E. Hernandez, *Physical Review B* **66**, 235415 (2002).
- [36] A. Dietrich, M. Brk, E. S. Steiger, L. Antoniuk, T. T. Tran, M. Nguyen, I. Aharonovich, F. Jelezko, and A. Kubanek, (2018).
- [37] W. J. Yu, W. M. Lau, S. P. Chan, Z. F. Liu, and Q. Q. Zheng, *Physical Review B* **67**, 014108 (2003).
- [38] M. Goldman, *Physical Review Letters* **114** (2015), 10.1103/PhysRevLett.114.145502.
- [39] Z. Shotan, H. Jayakumar, C. R. Considine, M. Mackoite, H. Fedder, J. Wrachtrup, A. Alkauskas, M. W. Doherty, V. M. Menon, and C. A. Meriles, *ACS Photonics* **3**, 2490 (2016).
- [40] A. Beveratos, R. Brouri, J.-P. Poizat, and P. Grangier, arXiv:quant-ph/0010044 (2000), arXiv: quant-ph/0010044.
- [41] A. L. Exarhos, D. A. Hopper, R. N. Patel, M. W. Doherty, and L. C. Bassett, arXiv:1804.09061 [quant-ph] (2018), arXiv: 1804.09061.
- [42] J. M. Binder, A. Stark, N. Tomek, J. Scheuer, F. Frank, K. D. Jahnke, C. Müller, S. Schmitt, M. H. Metsch, T. Unden, T. Gehring, A. Huck, U. L. Andersen, L. J. Rogers, and F. Jelezko, *SoftwareX* **6**, 85 (2017).
- [43] L. H. Li and Y. Chen, *Advanced Functional Materials* **26**, 2594 (2016), arXiv: 1605.01136.